Widely tunable type-II interband cascade laser

Sergey Suchalkin, Mikhail V. Kisin, Serge Luryi, and Gregory Belenky[a]
Department of Electrical & Computer Engineering, SUNY at Stony Brook, New York 11794

Fred J. Towner and John D. Bruno
Maxion Technologies Inc., Hyattsville, Maryland 20782

Carlos Monroy and Richard L. Tober
Army Research Lab, Adelphi, Maryland 20873

We discuss an ultrawide, voltage-tunable type-II mid-IR interband cascade laser. Its design has a charge accumulation layers outside of the optically active quantum wells that unclamps the electron-hole concentrations and facilitates above-threshold Stark shifts. Our results demonstrate laser tuning of 120 nm (120 cm^{-1}). © *2006 American Institute of Physics.*
[DOI: 10.1063/1.2165289]

Tunable semiconductor mid-IR lasers are in high demand for various military and civilian applications, such as free space communication, remote sensing, and environmental monitoring. Electrical tuning is the most direct and robust method of changing the emission wavelength and provides the fastest time response and the finest wavelength adjustment. Two methods of the electrical tuning are often employed in tunable laser design: injection current control of the modal refractive index,[1,2] and direct alteration of the laser emission wavelength by an external electric field (Stark effect).[3–6] The former approach is capable of single-mode tuning that ideally is limited by the spectral width of the material gain. The Stark effect, on the other hand, can provide electrical tuning of the spectral position of the whole gain curve. Above the lasing threshold, however, both methods are severely suppressed by concentration pinning in the laser active region, so that the Stark-effect tuning becomes noneffective and cannot be used practically without imposing significant complications to the laser structure, including, for example, multisectioned waveguide designs[1,5] and the necessity of longitudinal or vertical section integration.

This significant limitation can be avoided by separating the injected carriers into two groups: one that produces the radiation, and the other, accumulated outside the optically active layers, that serves as the source of the controlling electric field. In an earlier work,[6] this was accomplished by introducing two additional (electron and hole) accumulation quantum wells grown on both sides of an active type-I quantum well in a diode laser. A significant drawback of the device, however, was its narrow range of tunability (5 nm) due to the small second-order Stark shift of the energy levels in type-I quantum wells.[6] In this letter, we propose to employ type-II interband cascade structures which are characterized by an inherently strong first-order Stark effect. Indeed, in a type-II structure, the recombining electrons and holes are spatially separated, so that there is a nonzero dipole moment in the structure's growth direction even in the absence of the external electric field. Our tunneling-limited injection scheme with a charge accumulation layer outside the optically active type-II heterojunction unclamps the electron-hole concentrations in the active region and allows for an ultrawide tunable Stark shift of the laser emission even after the laser threshold has been reached.

Each period of the tunable laser cascade structure has four separate regions: a digitally graded injector, an (electron) accumulation quantum well, a tunnel barrier, and an optically active type-II heterojunction (see Fig. 1). These regions are designed consistently with one another, so that the emission wavelength depends on the bias current as follows. As the injection current increases above threshold, electrons start accumulating in the superlattice injector well adjacent to the tunnel barrier. (Their concentration determines the tunneling rate into upper energy level E_2 of the electron quantum well 2 shown in Fig. 1). Concurrently, injected holes accumulate in the hole quantum well 1. This charge separation results in an electric field (perpendicular to the epilayers) that increases with the injection current. The energy level positions E_{21} and, hence, the emission wavelength λ become dependent on the bias current which controls the electric field via charge accumulation.

The separation of the charge accumulation layers from the active region[6] enables the wavelength tuning above the laser threshold. At the current densities $J \geqslant J_{th}$, the maximum net modal optical gain is zero:
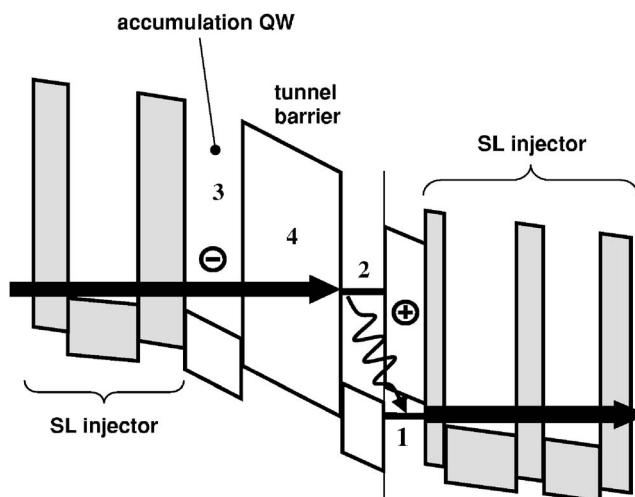

FIG. 1. Schematic band diagram of a single period of the IC laser structure under a bias voltage.

---

[a]Electronic mail: garik@ece.sunysb.edu

$$g_m^{\max} \equiv G_0\left[1 - \exp\left(-\frac{n_2^{(c)}}{N_{2D}}\right) - \exp\left(-\frac{n_1^{(h)}}{P_{2D}}\right)\right] - \alpha = 0, \tag{1}$$

where $n_2^{(c)}$ is the electron concentration in the electron quantum well, $n_1^{(h)}$ is the hole concentration in the hole well, $N_{2D} = kTm_e^*/\pi\hbar^2$ and $P_{2D} = kTm_h^*/\pi\hbar^2$ are effective two-dimensional (2D) densities of states in the conduction and the valence subbands, G_0 is the saturation gain and α is the optical loss.[7] The concentration in the electron accumulation layer 3 can be estimated in a steady-state regime by $n_3^{(c)} = J\tau_{\text{tun}}/q$, where τ_{tun} is the tunneling time and q is the electron charge. Using the charge neutrality condition, $n_1^{(h)} = n_3^{(c)} + n_2^{(c)}$, the electron concentration in the active quantum well is related to the injection current density J by the equation

$$\exp\left(-\frac{n_2^{(c)}}{N_{2D}}\right) + \exp\left(-\frac{n_2^{(c)} + J\tau_{\text{tun}}/q}{P_{2D}}\right) = 1 - \frac{\alpha}{G_0}. \tag{2}$$

Note, that as the current density increases above threshold, the electron concentration, $n_2^{(c)}$, in the optically active quantum well (#2 in Fig. 1) slightly decreases and finally saturates at a value determined by the optical loss, temperature, and material constants. On the other hand, the concentration in the electron accumulation layer $n_3^{(c)}$ increases with the current, as does the hole concentration, thus providing the overall charge neutrality and modal gain pinning together with the increase of the electric field in the active type-II heterojunction region. The latter, in turn, effects the laser wavelength tuning above threshold.

The tunable interband cascade (IC) laser structure was grown by molecular beam epitaxy on p-doped GaSb substrates. The active region of the laser is a cascade of 14 periods. Each period includes a digitally graded InAs/AlSb injector and InAs/Ga$_{0.8}$In$_{0.2}$Sb/GaSb type-II heterostrucure, separated by a 4 nm AlSb barrier. The widths of the InAs and Ga$_{0.8}$In$_{0.2}$Sb layers are 2.1 and 3.1 nm, respectively. The active area is sandwiched between InAs/AlSb superlattice claddings. The Ga$_{0.8}$In$_{0.2}$Sb layer is followed by a p-doped 5.8 nm GaSb QW which serves as a hole reservoir. The devices are fabricated as deep-etched mesas and soldered, epilayer side up, to Au-coated copper mounts. The mesas 35 μm wide with 0.5 mm long cavity lengths with both facets left uncoated. The mounts were attached to the cold finger of a liquid N$_2$ or He train cryostat. The emission was collected with the reflection optics and analyzed with an Fourier transform infrared spectrometer. We compared the tuning characteristics of this structure with those of a regular 18-cascade IC laser.[8] The latter had an active region with type-II W-like quantum wells and contained no special tunnel barriers for charge accumulation.

The experimental turn-on voltage is $\sim$5.2 V and agrees well with the theoretical prediction (4.9 V) for an ideal 14-period cascade structure. Calculation shows that 0.35 V voltage drop per each injector region provides for injector level alignment. For 56 nm injectors this corresponds to the turn-on internal electric field of about 65 kV/cm. The width of the tunnel barrier 4 in our design was chosen to be 4 nm, which ensures the alignment of the accumulation level 3 and upper lasing level 2 at turn-on voltage (see Fig. 1). The observed threshold current density is 91 A/cm^2 at 80 K. The lasers demonstrates cw operation up to 120 K and pulsed operation up to 200 K (pulse duration=400 ns, duty cycle
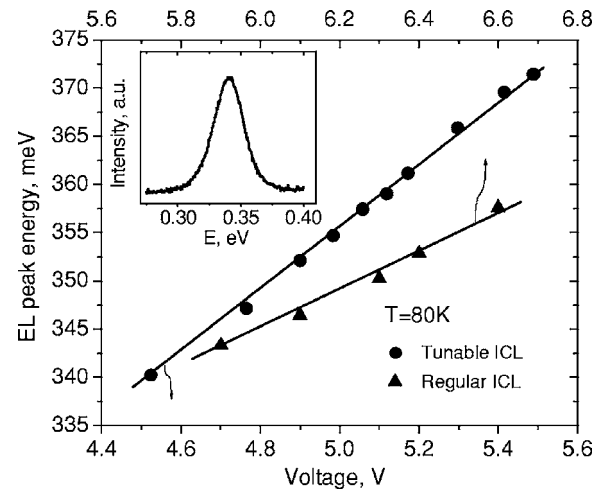

FIG. 2. The dependence of the EL quantum energy on the bias voltage for a regular IC laser (triangles) and tunable IC laser (circles). The inset shows the EL spectrum at low bias current.

=2.4%). The external quantum efficiency is $\sim$250% (80 K). The internal loss measured with Hakki-Paoli techniques is $\sim$10 cm^{-1}.

The electroluminescence (EL) spectrum at low current is shown in the inset of Fig. 2. The emission quantum energy is 0.34 eV agrees with the theoretical prediction (0.32 eV). The EL spectral maximum energy increases linearly with the bias voltage. Since the dependence is measured in the subthreshold pumping region, the linear shift can be attributed to the Stark effect that results from charge accumulation in the type-II quantum wells of the laser active area. A similar effect has been observed in a regular interband cascade laser (see Fig. 2). The effect is weaker in a regular IC laser due to the lower sensitivity of subband energies in a W-like quantum well with respect to charge accumulation.

Amplified spontaneous emission (ASE) and lasing spectra of both the tunable and the regular IC lasers are shown in Fig. 3. In the regular laser, in spite of the ASE blue shift, the laser line spectral position is stable up to high bias currents ($\sim$220$\times$ threshold values). This is as expected from the pinning of concentration and, hence, of electric field in the active area quantum wells. The lasing spectrum of the tunable laser [see Fig. 3(a), three upper curves] demonstrates a clear blueshift. The periodic modulation of the ASE spectrum in the tunable laser is attributed to optical mode leakage into the substrate.[9] This is consistent with the observed strong modulation of the modal gain spectrum with the same period [see Fig. 3(a), inset]. The spectral positions of the gain maxima and minima are determined by the substrate thickness as well as the effective refraction indices of the active area, claddings, and substrate. The dependence of these positions on the bias current is weaker than the direct Stark shift of the gain spectrum. As the bias current increases, the material gain curve shifts with respect to the modulation extremes and, consequently, the modal gain maximum shows a discrete blueshift with the increment equal to the leaky mode modulation period. This behavior takes place at the pumping level far higher than the laser threshold. The lasing spectrum of the tunable laser demonstrates a clear blueshift at increasing bias current. The rate of this shift with respect to the bias current (and voltage) is slower than the rate of ASE tuning in the subthreshold region (approximately 5 versus
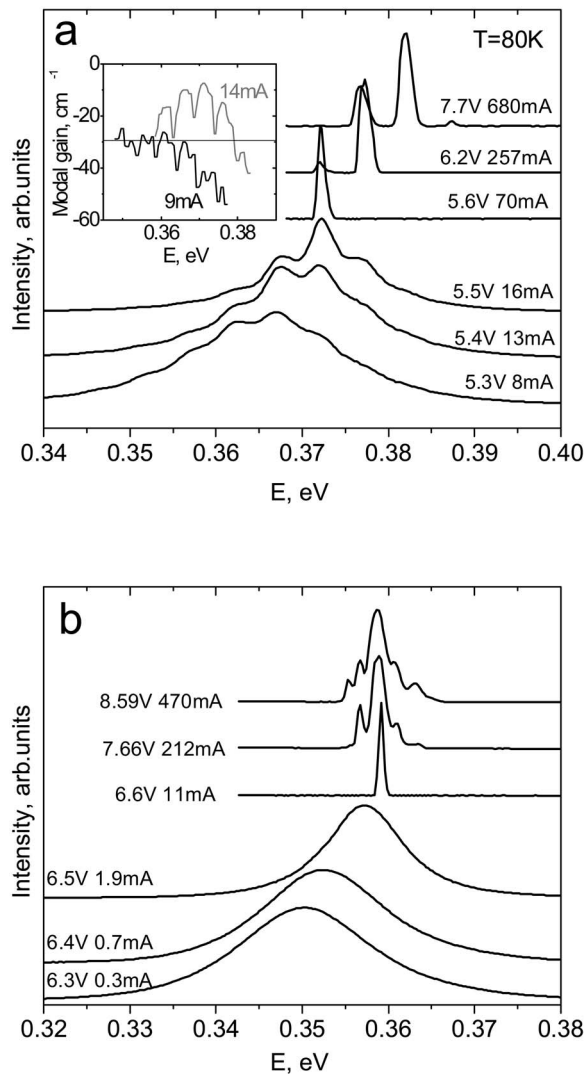
FIG. 3. ASE and laser spectra of the tunable IC laser (a) and regular IC laser (b) at different bias currents. The inset in the panel (a) shows the modal gain spectrum of the tunable IC laser.

FIG. 4. Lasing spectra of the tunable IC laser at different values of the injection current.

30 meV/V). This indicates an abrupt change in the tuning mechanism as the bias current exceeds the laser threshold. In the subthreshold regime, the wavelength shift is determined primarily by the carrier accumulation in the optically active quantum wells and is related to the corresponding increase of the internal electric field in the type-II heterojunction. After the laser threshold has been reached, the wavelength tuning becomes determined by the charge buildup in accumulation quantum well 3, which, in turn, depends on the electron tunneling rate through barrier 4. The change in the tuning rate above the threshold indicates that, in the present design, the rate of charge accumulation in quantum well 3 is lower than that in the optically active quantum wells below the threshold. Figure 4 demonstrates the laser spectrum shift recorded throughout the whole range of the injection current (1–42 threshold values) without noticeable saturation. The maxi-
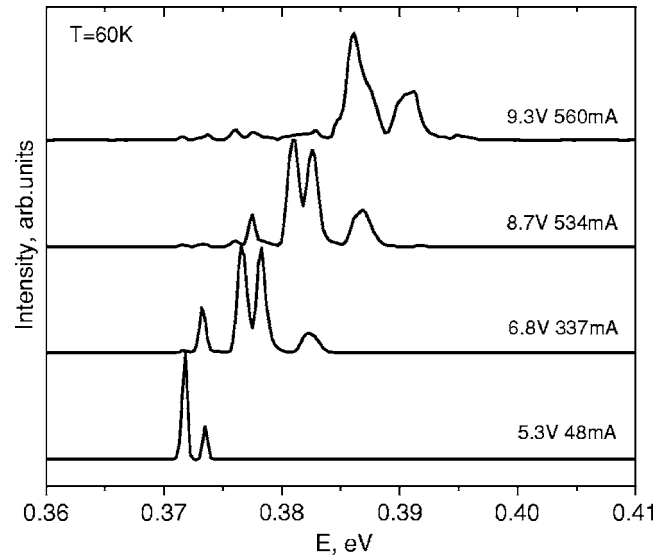
mum value of the laser emission tuning range is 15 meV or 120 nm.

In conclusion, we have demonstrated an electrically tunable interband cascade laser that operates in the mid-IR spectral range. The laser design includes an additional charge accumulation layer located outside the optically active quantum wells. This eliminates the electron-hole concentration pinning and thus enables an ultrawide Stark shift of the optical gain spectrum. The tuning range of our device is 120 nm (starting from the initial lasing wavelength λ ~ 3.33 μm), or 120 cm^{-1}. We believe the laser tuning performance can be further improved by suppressing the gain spectrum modulation due to the substrate leaky modes.

[1] L. A. Coldren and S. W. Corzine, IEEE J. Quantum Electron. **QE-23**, 903 (1987).
[2] S. Kobayashi, Y. Yamamoto, M. Ito, and T. Kimura, IEEE J. Quantum Electron. **QE-18**, 582 (1982).
[3] K. Ploog and G. H. Dohler, Adv. Phys. **32**, 285 (1983).
[4] H. Kroemer and G. Griffiths, IEEE Electron Device Lett. **EDL-4**, 20 (1983).
[5] J. Faist, F. Capasso, C. Sirtori, D. L. Sivco, A. L. Hutchinson, and A. Y. Cho, Nature (London) **387**, 777 (1994).
[6] N. Le Thomas, N. T. Pelekanos, Z. Hatzopoulos, E. Aperathitis, and R. Hamelin, Appl. Phys. Lett. **83**, 1304 (2003).
[7] V. B. Gorfinkel and S. Luryi, J. Lightwave Technol. **13**, 252 (1995).
[8] J. L. Bradshaw, N. P. Breznay, J. D. Bruno, J. M. Gomes, J. T. Pham, F. J. Towner, D. E. Wortman, R. L. Tober, C. J. Monroy, and K. A. Olver, Physica E (Amsterdam) **20**, 479 (2004).
[9] D. Westerfeld, S. Suchalkin, M. Kisin, G. Belenky, J. Bruno, and R. Tober, IEE Proc.: Optoelectron. **150**, 293 (2003).